



Intestinal tube formation in *Caenorhabditis elegans* requires *vang-1* and *egl-15* signaling

Michael Hoffmann^{b,c,1}, Christoph Segbert^{b,1}, Gisela Helbig^b, Olaf Bossinger^{a,*}

^a Institute of Molecular and Cellular Anatomy (MOCA), RWTH Aachen University, D-52074 Aachen, Germany

^b Institute for Genetics, Heinrich-Heine-University Düsseldorf, D-40225 Düsseldorf, Germany

^c Department of General Pediatrics, Heinrich-Heine-University, D-40225 Düsseldorf, Germany

ARTICLE INFO

Article history:

Received for publication 12 June 2009

Revised 26 November 2009

Accepted 1 December 2009

Available online 11 December 2009

Keywords:

Caenorhabditis elegans

Cell intercalation

Epithelium

FGF signaling

Intestine

Organogenesis

Intercellular junctions

Planar cell polarity

Wnt signaling

ABSTRACT

Understanding how epithelial organs form during morphogenesis is a major problem in developmental biology. In the present paper, we provide a detailed analysis of *vang-1*, the only homolog of the planar cell polarity protein Strabismus/Van Gogh in *Caenorhabditis elegans*. We demonstrate that during organogenesis of the intestine, (i) VANG-1 specifically interacts with PDZ 2 domain of DLG-1 (Discs large) and becomes phosphorylated by the kinase domain of the FGF-like receptor tyrosine kinase EGL-15; (ii) VANG-1 is predominantly restrained to the cell cortex but relocates to the apical junction; and (iii) in *vang-1* embryos epithelial cells of the intestine are not correctly arranged along the anterior–posterior axis. To investigate what determines the disposition of the VANG-1 protein, either truncated protein forms were expressed in the intestine or RNAi was used to remove the functions of gene products previously shown to be involved in apical junction formation. Removal of the VANG-1 PDZ binding motif “–ESAV” and depletion of *dlg-1* or *let-413* gene functions interferes with the localization of VANG-1. In addition, *egl-15* embryos show a premature relocation of VANG-1 to the apical junction, causing defects that resemble those observed in mutant *vang-1* embryos and after intestine-specific overexpression of full-length *vang-1*. Finally, the localization of VANG-1 depends on DSH-2, a homolog of the planar cell polarity protein Dishevelled and depletion phenocopies *vang-1* and *egl-15* phenotypes in the embryonic intestine.

© 2010 Elsevier Inc. All rights reserved.

Introduction

The PCP pathway is highly conserved from *Drosophila* to vertebrates (Wang and Nathans, 2007; Wu and Mlodzik, 2009). The developmental function of this pathway is to mediate the coordinated orientation of cells or structures within the plane of an epithelium (e.g. in the *Drosophila* compound eye) or to regulate the organization of cellular intercalation that is required for morphogenesis (e.g. neural tube formation in mouse). Recent analysis of organ development showed that the PCP component Van Gogh/VANG-1 is involved in tissue polarity of the egg-laying system and asymmetric B cell division in *Caenorhabditis elegans* (Green et al., 2008; Park et al., 2004; Wu and Herman, 2006, 2007) but a detailed analysis of VANG-1 is missing so far. The *C. elegans* intestine provides another simple and accessible model system to study organogenesis (Hermann et al., 2000; Leung et al., 1999; McGhee, 2007; Sulston et

al., 1983). The mature intestine is assembled by just twenty cells which are arranged in an invariant and easily reproducible pattern that is generally achieved by the intercalation of a specific set of cells (Leung et al., 1999). The signaling events that regulate distinct intercalation events in the intestinal primordium are still poorly understood. During the intercalation process the symmetry of the intestinal primordium changes from radial to bilateral and a relatively long tube is made from a small number of cells (Leung et al., 1999). Well-characterized examples of cell intercalation can be found in *Drosophila* and *Xenopus* (Bertet et al., 2004; Keller et al., 2008; Wallingford et al., 2002). Basically, the morphogenetic processes described in these organisms demonstrate convergence and extension of cells that finally lead to an elongation of tissues/organs along the axis of the embryo. This mediolateral cell intercalation is regulated by the noncanonical wnt/PCP pathway (Keller, 2002). One of the core members of the PCP pathway is the four-pass transmembrane protein Strabismus/Van Gogh, first identified in *Drosophila* (Taylor et al., 1998; Wolff and Rubin, 1998). Interference of the PCP pathway leads to misorganization of affected epithelia, e.g. in *Xenopus* the depletion of *XStbm* function by RNAi impairs axial elongation (Darken et al., 2002).

Here we provide a detailed molecular and functional analysis of *C. elegans vang-1*, the homolog of the *Drosophila* PCP gene *strabismus/Van Gogh*. *vang-1* is involved in organogenesis, where it mediates the

Abbreviations: CeAJ, *Caenorhabditis elegans* apical junction; DAC, DLG-1–AJM-1 complex; mab, monoclonal antibody; PCP, planar cell polarity; PDZ (PSD95, Discs large, ZO-1); RNAi, RNA-mediated interference; RT, room temperature; Y2HA, yeast two-hybrid analysis; WT, wild type.

* Corresponding author. Fax: +49 241 808 2508.

E-mail address: olaf.bossinger@rwth-aachen.de (O. Bossinger).

¹ These authors equally contributed to this work.

proper arrangement of epithelial cells within the intestinal tube. VANG-1 physically interacts with the apical junctional molecule DLG-1 (Discs large) and becomes a component of the CeAJ during embryonic development. The proper subcellular localization of VANG-1 also requires the function of LET-413, DLG-1, the FGF-like receptor tyrosine kinase EGL-15 and the PDZ domain protein DSH-2 (Dishevelled related).

Materials and methods

C. elegans strains and alleles

Maintenance and handling of *C. elegans* were carried out as described previously (Brenner, 1974). Bristol N2 was used as the WT strain. The following mutant strains were used: *vang-1(tm1422)* and *egl-15(n1456)* (<http://wormbase.org>).

Molecular analysis of *vang-1*

VANG-1 corresponds to the predicted open reading frame B0410.2, which is located on chromosome X (see <http://wormbase.org> for further information). The predicted sequence was verified by sequencing cloned full-length RT-PCR product from mixed stage poly-A⁺ RNA by using the one step RT-PCR kit (Qiagen) and the following primers:

forward 5'-GTGCCGGGGTACCTCGTATCAAG-3',
reverse 5'-CCCACGGTACCACTGCCGACTC-3'

(synthetic restriction sites for *KpnI* are underlined).

The same primers were used to sequence mutant alleles of *vang-1* (see below).

Immunostaining of embryos

Gravid adults were transferred with a drawn-out pipette to a microscope slide coated with a thin layer of polylysine in a drop of sterile dH₂O and cut with a scalpel. Embryos were immediately permeabilized by the freeze-crack method (Strome and Wood, 1983) and fixed in 100% methanol (10 min), 100% acetone (20 min), 90% ethanol (10 min), 60% ethanol (10 min) and 30% ethanol (10 min). Slides were washed twice for 10 min each with TBT [Tris-buffered saline (25 mM Tris), plus 0.1% Tween 20 or Triton X-100], incubated at 4 °C overnight with primary antibodies (see below) in blocking buffer (TBT plus 1% bovine serum albumin and 1% nonfat dry milk powder), washed three times for 10 min each with TBT at RT and incubated at RT for 1–3 h, with secondary antibodies (see below) in blocking buffer. Finally, slides were washed three times for 10 min each in TBT and mounted in Mowiol containing 1,4-diazabicyclo(2.2.2)octane (Sigma-Aldrich) as an antifade reagent. The following primary and secondary antibodies were diluted in blocking buffer: mabMH27 (Hybridoma Bank, Iowa City, IA), anti-VANG-1 (rabbit, see also below), anti-DLG-1 (rabbit) (Segbert et al., 2004), anti-DSH-2 (rabbit) (Hawkins et al., 2005) and anti-GFP (mouse, 1:100, Sigma). Secondary antibodies were Cy2, Cy-3 (1:200; Jackson ImmunoResearch Laboratories, West Grove, PA) and Alexa 647 (1:200; Molecular Probes) conjugated. YoYo-1 (1:20,000; Molecular Probes) and RNase A (1:200; 10 µg/µl) were added with secondary antibodies for DNA staining.

Because RNAi against *vang-1* gene function did not recapitulate the *vang-1(tm1422)* phenotype (Fig. 7) and a deficiency removing the *vang-1* locus was not available (<http://www.wormbase.org>), the specificity of polyclonal anti-VANG-1 antibodies was tested as follows: (a) the VANG-1 expression pattern (Figs. 3 and 5) is not detectable with the pre-immunoserum (not shown); (b) incubation of anti-VANG-1 antibodies (30 min, RT) in blocking solution with an

excess of 6× His-tagged VANG-1 protein (0.5–1 µg/µl) prior to usage on fixed *C. elegans* embryos produced a strongly reduced staining pattern (not shown); and (c) overexpression of full-length VANG-1 under the control of the intestine-specific *elt-2* promoter (Fukushige et al., 1998) resulted in an enhanced anti-VANG-1 staining pattern at the cell cortex (Fig. 5A) in comparison to WT embryos (Fig. 3B). Hence, we conclude that our polyclonal anti-VANG-1 antibodies recognize VANG-1 protein.

Immunofluorescence analysis of embryos was performed on a confocal laser microscope (LSM-Meta 510, Zeiss). As not stated otherwise, recorded images represent a Z-projection of optical sections taken 0.5 µm apart.

VANG-1 antibody production

PCR was used to amplify a 984-bp fragment, encoding the C-terminal 328 aa of VANG-1 (FERY...ESAV; see Fig. S4):

forward: 5'-TGTCAGGGGATCCTTTGAAAGATAC-3',
reverse: 5'-CTAGCCGGTACTCAAACCTGCCGAC-3'

(synthetic restriction sites for *BamHI* and *KpnI* are underlined).

The fragment was cloned in frame in the 6× His-tag expression vector pQE30 (Qiagen), transformed and induced in *E. coli* strain M15 [pREP4] (Qiagen). Recombinant protein was purified on Ni²⁺-NTA matrix (Qiagen) and sent to Eurogentec (Seraing, Belgium) for immunization. The final bleed of one rabbit was purified using blot overlay technique and the recombinant protein as a bait. For elution of anti-VANG-1 antibodies, 0.5 mm blot stripes were rinsed with 400 µl Glycine (100 mM, pH 2.5) and collected in 100 µl Tris-Cl (pH 8.0).

RNAi

RNAi by feeding was done, performed as described by others (Kamath et al., 2001). The following fragments were cloned between the T7 promoters of the pPD129.36 (L4440) feeding vector: *dlg-1*, a 1.5-kb *XhoI* fragment of *yk128b7*; *let-413* a 2.5-kb *XbaI* fragment of *yk524b7*; and *vang-1* full-length RT-PCR product (see above). The RNAi clone for *dsh-2* was obtained from the Ahringer RNAi Library (Geneservice Limited, UK). The recombinant plasmid was transformed into the RNase III-deficient *E. coli* strain HT115 (DE3), carrying IPTG-inducible T7 polymerase. After amplification of a single colony overnight (37 °C, LB_{amp tet} medium), bacteria were seeded on NGM_{amp tet} plates, containing IPTG (1 mM) and further incubated overnight at RT to allow the expression of dsRNA. The 10–20 WT embryos were transferred to a single plate and allowed to grow to adulthood (15 °C), and their offspring were analyzed. RNAi was also done by injection. After *in vitro* transcription (RiboMax, Promega, Madison, WI), dsRNA diluted to a final concentration of 0.5 µg/µl was injected into the gonads of young adult WT hermaphrodites (maintained at 15 °C). After 24–48 h, the progeny of injected worms were prepared for antibody staining.

Pull-down assay

A bacterially expressed 6× His-tagged 1170-bp fragment encoding PDZ domains 1–3 of DLG-1 (aa 204–593, VLEK...RPQE) was coupled to Ni²⁺-NTA matrix (Qiagen) and washed 4 times with TNT (50 mM Tris-Cl pH 8.0, 150 mM NaCl, 1% Tx-100). Then, 10 µl of an *in vitro* transcribed/translated and biotinylated 984-bp fragment encoding 328 aa of VANG-1 (FERY...ESAV; see Fig. S4) was added together with 100 µl TNT containing 1 mg/ml BSA and 0.25 µl freshly prepared protease inhibitor cocktail (500 µg/ml aprotinin, 500 µg/ml leupeptin, 500 µg/ml pepstatin), incubated for 4 h with rotation at 4 °C and washed again 4 times with TNT. The sample was then boiled in 2× SDS for 10 min, chilled on ice for 5 min and frozen in liquid

nitrogen for 10 min. Afterwards, the sample was loaded on a 10% SDS-polyacrylamide gel. Separated proteins were transferred to nitrocellulose membrane, incubated with blocking buffer containing TBT for 1 h at RT, further incubated at 4 °C overnight with rabbit anti-DLG-1 antibodies (1:200, see above) in blocking buffer (without sodium azide), washed three times for 5 min each with TBT at RT and finally incubated at RT for 1.5 h with anti-rabbit secondary antibody (HRP conjugated, 1:10,000) in blocking buffer (without sodium azide). After washing three times for 5 min each in TBT, detection was performed using BM chemiluminescence substrate. The membrane was incubated with TBT blocking buffer again (sodium azide irreversibly inactivates HRP) and re-probed with Streptavidin-HRP (1:200, Molecular Probes) in blocking buffer.

Co-immunoprecipitation

Frozen 500 µl worm pellets were crunched by using mortar and pestle. The resulting worm powder was transferred to a reaction tube and 1 ml of TNT buffer containing protease inhibitors (see above) was added. After vortexing for 5 min, the solution was kept on ice for 30 min and centrifugated at 4 °C for 15 min. The supernatant was transferred into a new reaction tube and washed twice by centrifugation at 4 °C for 15 min. For each experiment, 1 mg of protein extract was used. Lysates were preincubated with protein A agarose beads (Biotechnology) for 1 h at 4 °C on a rotating platform. Following centrifugation (12,000 rpm, 4 °C, 2 min), the supernatant was either incubated with anti-GFP antibodies (rabbit, 1:1000) or anti-peptide antibodies against VANG-1 (rabbit, 1:1000; Eurogentec; targeted amino acids 51–65: SEGQKIAPPNEDWAD) for 2 h at 4 °C on a rotating platform. After addition and incubation with protein A agarose beads, beads were washed with TNT buffer three times. SDS-PAGE and western blot analyses were carried out as described above, using anti-rabbit secondary antibody (HRP conjugated, 1:5000).

Kinase assay

A bacterially expressed 6× His-tagged 328 aa fragment encoding C terminus of VANG-1 (FERY...ESAV; see Fig. S4) was incubated with *in vitro* transcribed/translated EGL-15 kinase domain (see below) for 20 min at RT in freshly prepared 1× kinase buffer (see below). Then 5 µl Ni²⁺-NTA was added, incubated for 15 min at RT and washed 4 times with TNT. The sample was then boiled in 2× SDS for 10 min, chilled on ice for 5 min and frozen in liquid nitrogen for 10 min. Afterwards, SDS-PAGE and western blot were performed as described above. The following antibodies were used in this assay: anti-phosphotyrosine (mouse, 1:100, Invitrogen) and anti-tetra His (mouse, 1:2000, Qiagen). Kinase buffer (5×): 50 mM MgCl₂, 5 mM MnCl₂, 5 mM DTT, 1 mM ATP and 100 mM Tris-Cl pH 7.4.

Primers used for cloning of EGL-15 kinase domain encoding 1481-bp fragment (CKQT...KPEF) into pGBKT7 vector (Clontech):

forward 5'-GTCCATGGTGTGCAAAACAACACTAC-3',
reverse 5'-CTAACTGCAGTCAAAATTCGGGT-3'

(synthetic restriction sites for NcoI and PstI are underlined).

Yeast two-hybrid analysis

A 1170-bp fragment of the *dlg-1* cDNA corresponding to amino acids 204–593 (VLEK...RPQE) that contains all three PDZ domains was cloned into GAL4 DNA-binding domain vector pGBKT7 (Clontech) using the following primer:

forward 5'-AGGAATTCGTCCTTGGAGAAAGGTCAC-3',
reverse 5'-ATGGATCCCTCTTGTGCTGTACTG-3'

(synthetic restriction sites for EcoRI and BamHI are underlined).

This bait was used to screen ~2.5 million colonies of an embryonic cDNA library (kindly provided by Dr. Zheng) in the GAL4 transcriptional activation domain vector pACT2 (Clontech). Interacting clones were selected for activity of the HIS3, ADEX and *lacZ* genes. For fine mapping of the VANG-1–DLG-1 interaction, the following primers were used to amplify and clone DLG-1 single PDZ domains and combinations of PDZ domains into the pGBKT7 vector:

PDZ 1 (381-bp fragment, VLEK...PSAP):

forward 5'-AGGAATTCGTCCTTGGAGAAAGGTCAC-3',
reverse 5'-TGGTGGGATCCCGGAGCCGATGG-3'.

PDZ 2 (441-bp fragment, IHPP...DYNR):

forward 5'-TCCATCGGAATTCATTCATCCACC-3',
reverse 5'-TCCCATGGATCCGCGGTGTAG-3'.

PDZ 3 (348-bp fragment, SQMG...RPQE):

forward 5'-GACTACGAATTCTCTCAAATGG-3',
reverse 5'-ATGGATCCCTCTTGTGCTGTACTG-3'.

PDZ 1 + 2 (822-bp fragment, VLEK...DYNR):

forward: see PDZ 1,
reverse: see PDZ 2.

PDZ 2 + 3 (789-bp fragment, IHPP...RPQE):

forward: see PDZ 2,
reverse: see PDZ 3

(synthetic restriction sites for EcoRI and BamHI are underlined).

With regard to the analysis of Dishevelled–VANG-1 interactions, the following primers were used to amplify and clone the PDZ domains of DSH-1, DSH-2 and MIG-5 into the pGBT9 vector:

DSH-1 PDZ (490-bp fragment, GSTT...DTQA):

forward 5'-ATGATGAATTCGGCTCTACAACAAC-3',
reverse 5'-TTGGGATCCCTCATTCGATTCG-3'.

DSH-2 PDZ (398-bp fragment, FSSI...ATNA):

forward 5'-CTTCAGAATTCCTTTCAAGCATCAC-3',
reverse 5'-CATTGGATCCATAGCATTCTGTCG-3'.

MIG-5 PDZ (411-bp fragment, FRRP...GVVW):

forward 5'-GAAAGGGATCCTTCAGAAGACCGTATG-3',
reverse 5'-ACAGCCTGCAGTACCCAAACTCCAAC-3'.

(synthetic restriction sites for EcoRI, BamHI and PstI are underlined, respectively).

To clone the 984-bp fragment, encoding the C-terminal 328 aa of VANG-1 (FERY...ESAV) into the pACT2 vector (Clontech), the pQE30-VANG-1 construct (see antibody production) was used as a template and digested with BamHI. The pACT2-VANG-1ΔESAV construct was generated by PCR using the pQE30-VANG-1 construct as a template and the following primers:

VANG-1ΔESAV (975-bp fragment, FERY...KISN):

forward: 5'-TGTCAGGGATCCTTTGAAAGATAC-3',
reverse 5'-CAAACGGTACCCTAATTGCTAATTTT-3'

(synthetic restriction sites for BamHI and KpnI are underlined, respectively).

Molecular biology

Intestine-specific overexpression vector (pOLB10) was generated from pPD49.78 by excision of the *hsp16-2* promoter and following insertion of the *elt-2* promoter (kindly provided by J. McGhee) using EcoRV and KpnI. Full-length (FL) or truncated (Δ) *vang-1*

overexpression constructs were made by cloning PCR products into pOLB10 vector by using the following primers:

vang-1 FL (1596-bp fragment, MSYQ...ESAV):

forward 5'-GTGCCGGGTACCTCGTATCAAG-3',
reverse 5'-CCCACGGTACCAACTGCCGACTC-3'.

vang-1 ΔN (984-bp fragment, FERY...ESAV):

forward 5'-TGTCAGGGGTACCTTTGAAAGATAC-3',
reverse 5'-CCCACGGTACCAACTGCCGACTC-3'.

vang-1 ΔESAV (1585-bp fragment, MSYQ...KISN):

forward 5'-GTGCCGGGTACCTCGTATCAAG-3',
reverse 5'-CAAACGGTACCTAATTGCTAATTTT-3'

(synthetic restriction sites for *KpnI* are underlined).

vang-1 ΔC + GFP "+ESAV"

For this construct, we first subcloned a 717-bp fragment of *vang-1* (MSYQ...LELR) into the pBluescript II KS vector (Stratagene) using forward 5'-GTGCCGGGTACCTCGTATCAAG-3' and reverse 5'-CAGCGAATTCACGAAGCTCGAG-3' primers. Then the 720-bp GFP sequence

from pEGFP-N1 vector (Clontech) was cloned by PCR into the pBluescript-*vang-1* construct using

forward 5'-TCGAATTCATGGTGGAGCAAG-3' and
reverse 5'-GCGGATCCTTACTTGTACAGCTC-3'

(synthetic restriction sites for *EcoRI* and *BamHI* are underlined).

On the resulting construct, we used the following primers for PCR to clone a 1446-bp fragment (MSYQ...—GFP sequence—ESAV) into the pOLB10 vector:

forward 5'-TGGGTACCTCGTATCAAGATAACAG-3',
reverse 5'-CAGGTACCTCAAAGTCCGACTCCTTGTACAGCTCGTC-CAT-3'

(the synthetic restriction site for *KpnI* is underlined).

GFP + *vang-1* C terminus

The 720-bp GFP sequence from pEGFP-N1 vector was cloned without stop-codon by PCR into the pBluescript vector using forward 5'-TCGGATCCATGGTGAGCAAG-3' and reverse 5'-GCGGATCCCTTGTA-CAGCTCGTC-3'. The C terminus of VANG-1 (FERY...ESAV; the epitope for the production of polyclonal antibodies, see Fig. S4) was cloned

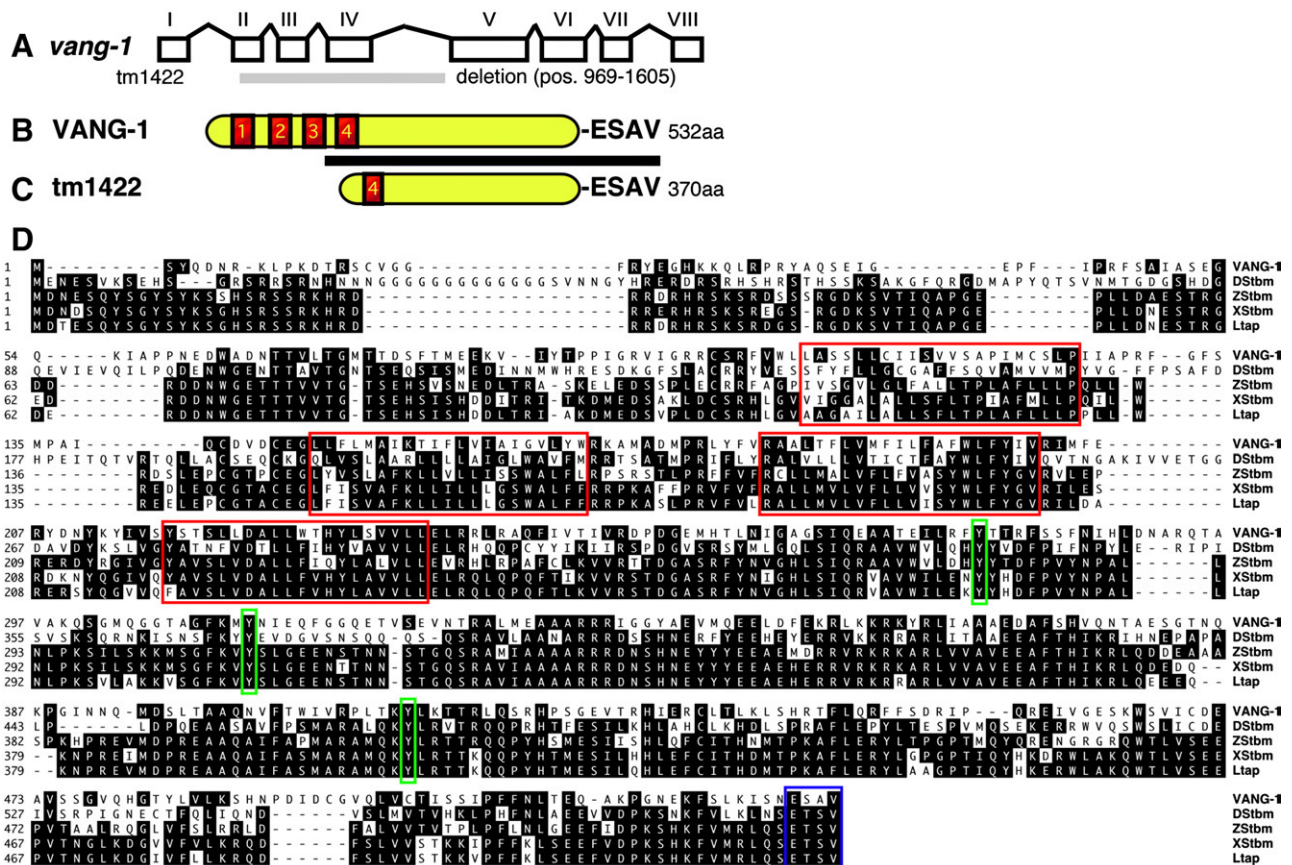


Fig. 1. Molecular characterization of *vang-1*, which encodes the *Caenorhabditis elegans* Strabismus/Van Gogh homolog. (A) Schematic illustration of the *vang-1* transcript (1599 nt; GenBank accession no. NM_076099). The *vang-1* gene contains eight exons and is trans-spliced to SL1 at the 5' end. AUG and UGA mark the translation initiation and termination codons, respectively. The 3'-UTR contains putative polyadenylation signals (AAAUA and AAUAUA) upstream (pos. 4955, 5063, 5130, 5170 and 7004 and 8319) of the poly-A tail. The gray bar marks the deleted region in *vang-1* (*tm1422*) (nt 969–1605 of genomic DNA, relative to the start codon; see also Figs. S2 and S3). (B) *vang-1* encodes a protein of 532 aa. The N terminus contains four predicted transmembrane domains: aa 101–127, aa 147–167, aa 179–201 and aa 213–236 (<http://www.ebi.ac.uk/Tools/phobius>; <http://www.cbs.dtu.dk/services/TMHMM>) (Krogh et al., 2001; Sonnhammer et al., 1998). The C terminus contains a consensus type I PDZ domain binding motif “–ESAV” (Songyang et al., 1997). The black bar marks the protein fragment used for generation of anti-VANG-1 antibodies (see also Fig. S4). (C) Sequencing of *vang-1* (*tm1422*) cDNA predicts a truncated protein form of 370 aa (aa 53–214 missing). (D) Sequence alignment of VANG-1, *Drosophila vang* (GenBank accession no. AAF58989), *Xenopus laevis strabismus* (GenBank accession no. AF427792) and mouse *vang-like 2* (GenBank accession no. AAK91927) reveals 26%, 28% and 26% identity (Lasergene; DNASTAR, Inc., WI, USA). The N-terminal transmembrane domains, conserved tyrosine residues, and the C-terminal consensus type I PDZ domain binding motif are boxed in red, green and blue, respectively.

into the resulting construct by PCR using pQE30-VANG-1 construct as a template and the following primers:

forward 5'-TGTCAGGGGATCCTTTGAAAGATAC-3',
reverse 5'-CCCACGGTACCAACTGCCGACTC-3'.

The resulting construct was used as a template to clone the GFP + vang-1 C terminus into the pOLB10 vector by PCR using the following primers:

forward 5'-TCGGTACCATGGTGAGCAAG-3'
reverse 5'-CCCACGGTACCAACTGCCGACTC-3'

(synthetic restriction sites for *Bam*HI are underlined).

Results and discussion

The *C. elegans* Strabismus/Van Gogh homolog VANG-1 interacts with DLG-1

The DAC plays a crucial role during the development of the CeAJ in all epithelia of *C. elegans*, analyzed so far (Carberry et al., 2009; Labouesse, 2006; Lynch and Hardin, 2009). In order to identify new binding partners of DLG-1 and to further analyze junction formation in *C. elegans*, we performed a Y2HA using PDZ domains 1–3, SH3 domain and GUK domain of DLG-1 as baits. After screening ~2.5 million yeast clones for each bait, one cDNA fragment, which was found two times, encodes a protein with a canonical PDZ binding motif “–ESAV” at its C terminus (Figs. 1A–D; see Fig. S1 for complete list of interacting partners). Database searches revealed that this sequence belongs to the predicted open reading frame B0410.2a/b that encodes a four-pass transmembrane protein with homology to the Strabismus/Van Gogh/Ltap proteins identified in *Drosophila*, *Xenopus* and vertebrates (Darken et al., 2002; Goto and Keller, 2002; Kibar et al., 2001). While *C. elegans* B0410.2a/b only shows moderate sequence similarities (Fig. 1D) to Strabismus/Van Gogh proteins in *Drosophila* (50%), *Xenopus* (51%) and mouse (52%), the overall domain architecture is very well conserved. Like in *Drosophila* and vertebrates, *C. elegans* B0410.2a/b contains four hydrophobic transmembrane domains at its N terminus and a consensus PDZ binding motif “–ESAV” at its C terminus (Fig. 1B). Additional BLAST searches revealed no other *C. elegans* proteins with homologies to B0410.2a/b, suggesting that B0410.2a/b is the only Strabismus/Van Gogh homolog in *C. elegans* and was therefore named VANG-1.

To map the interacting domain of VANG-1 and DLG-1 more precisely, we used Y2HA (Fig. 2). After fusion of the C terminus of VANG-1 to the GAL4 transactivation domain, either with or without the PDZ binding motif (aa 432–523: VANG-1^{+ESAV}; or aa 432–519: VANG-1^{–ESAV}), we tested for interaction with various PDZ constructs of DLG-1 fused to the GAL4 DNA-binding domain (Fig. 2A). As expected, the PDZ 1–3 fragment of DLG-1 interacts with VANG-1^{+ESAV}, while DLG-1 binding is abolished in case of using VANG-1^{–ESAV}. A more detailed analysis reveals that VANG-1^{+ESAV} interacts with PDZ 1–2 and PDZ 2–3 domains, but not with any of the individual PDZ domains. To test whether VANG-1 unspecifically interacts with PDZ domains in Y2HA, we used PDZ 1–3 domains of *Drosophila* Bazooka (Kuchinke et al., 1998; Wodarz et al., 1999). No interaction of VANG-1^{+ESAV} and Bazooka takes place (Fig. 2A), suggesting that the interaction of VANG-1 and DLG-1 is specific.

We further confirmed the interaction of VANG-1 and DLG-1 in pull-down experiments. Therefore, *in vitro* translated and biotinylated VANG-1^{+ESAV} or VANG-1^{–ESAV} proteins were incubated with bacterially expressed 6× His-tagged PDZ 1–3 fragments of DLG-1 and subjected to SDS-PAGE and Western analysis (Fig. 2B). While significant amounts of VANG-1^{+ESAV} were pulled down by the 6× His-tagged PDZ 1–3 fragments, no signal was detected in case of the VANG-1^{–ESAV} pull

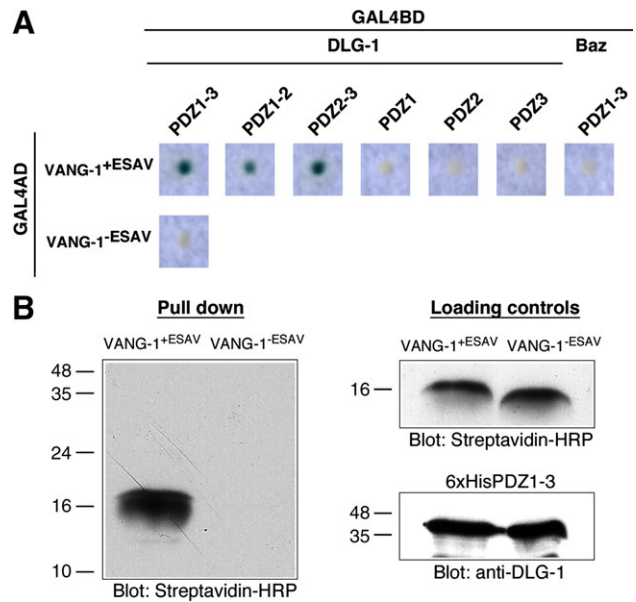


Fig. 2. VANG-1 physically interacts with DLG-1 *in vitro*. (A) Yeast two-hybrid analysis of VANG-1 using the C terminus fused to the GAL4 activation domain as a bait and different combinations of PDZ 1–3 domains of DLG-1 as preys (GAL4BD). Positive and negative interactions are indicated by blue and white colonies, respectively. *Drosophila* Bazooka (Baz) PDZ domains 1–3 was used as a negative control. Only combinations of at least two adjacent PDZ domains (e.g. PDZ 1–2 or PDZ 2–3) specifically interact with VANG-1^{+ESAV} but not with VANG-1^{–ESAV}. (B) Pull-down assay using His-tagged VANG-1 constructs and *in vitro* translated DLG-1 PDZ domains 1–3. The DLG-1 fragment is only pulled down by VANG-1^{+ESAV}. Loading controls confirmed that comparable amounts of proteins were used in both pull-down experiments.

down. In addition, the interaction of DLG-1 and VANG-1 proteins *in vivo* was confirmed by co-immunoprecipitation (Fig. S5).

These findings suggest that VANG-1 binds the PDZ domains of DLG-1 directly and the C-terminal PDZ binding motif of VANG-1 is necessary for DLG-1 interaction. The PDZ 2 domain of DLG-1 is necessary but not sufficient for VANG-1 binding suggesting that either upstream or downstream sequences of PDZ 2 domain are required for interaction. The direct interaction of VANG-1 and DLG-1 homologs *in vivo* has already been demonstrated in *Drosophila* and mammals, which gives further support to the idea that complex formation is evolutionary conserved (Bellaiche et al., 2004; Kallay et al., 2006; Lee et al., 2003).

Expression pattern of VANG-1 during embryonic development

To analyze the localization of VANG-1 during embryogenesis of *C. elegans*, we generated and affinity-purified rabbit polyclonal antibodies directed against the C-terminal 328 aa of VANG-1 (FERY...ESAV; see Fig. S4).

During morphogenesis of the intestine, VANG-1 exhibits a complex spatio-temporal subcellular localization pattern. At the onset of morphogenesis (Figs. 3A–a'), the expression of VANG-1 is detectable at the apical (arrow) and basolateral (arrowhead) domains of the intestinal epithelium. During more advanced morphogenesis, VANG-1 seems gradually to disappear from the apical membrane domain and becomes restricted to the basolateral domain (Figs. 3B–b', arrowhead). In later morphogenesis, VANG-1 predominantly localizes to the apex of intestinal cells (Figs. 3C–c'; arrow) and the staining pattern emerges in a structure, reminiscent to the CeAJ. Prior to hatching, most VANG-1 protein seems to localize at the CeAJ in the intestine (Fig. 3d; arrow). To test whether VANG-1 is indeed a component of the DAC, we performed double-labeling with anti-VANG-1 and anti-AJM-1 antibodies. Both proteins show a clear colocalization at the CeAJ in the intestine (Figs. 3D–d', arrows). These results are in line with the distribution of Strabismus/Van Gogh in *Drosophila*. During division of the sensory organ precursor cell the localization of Strabismus/Van Gogh

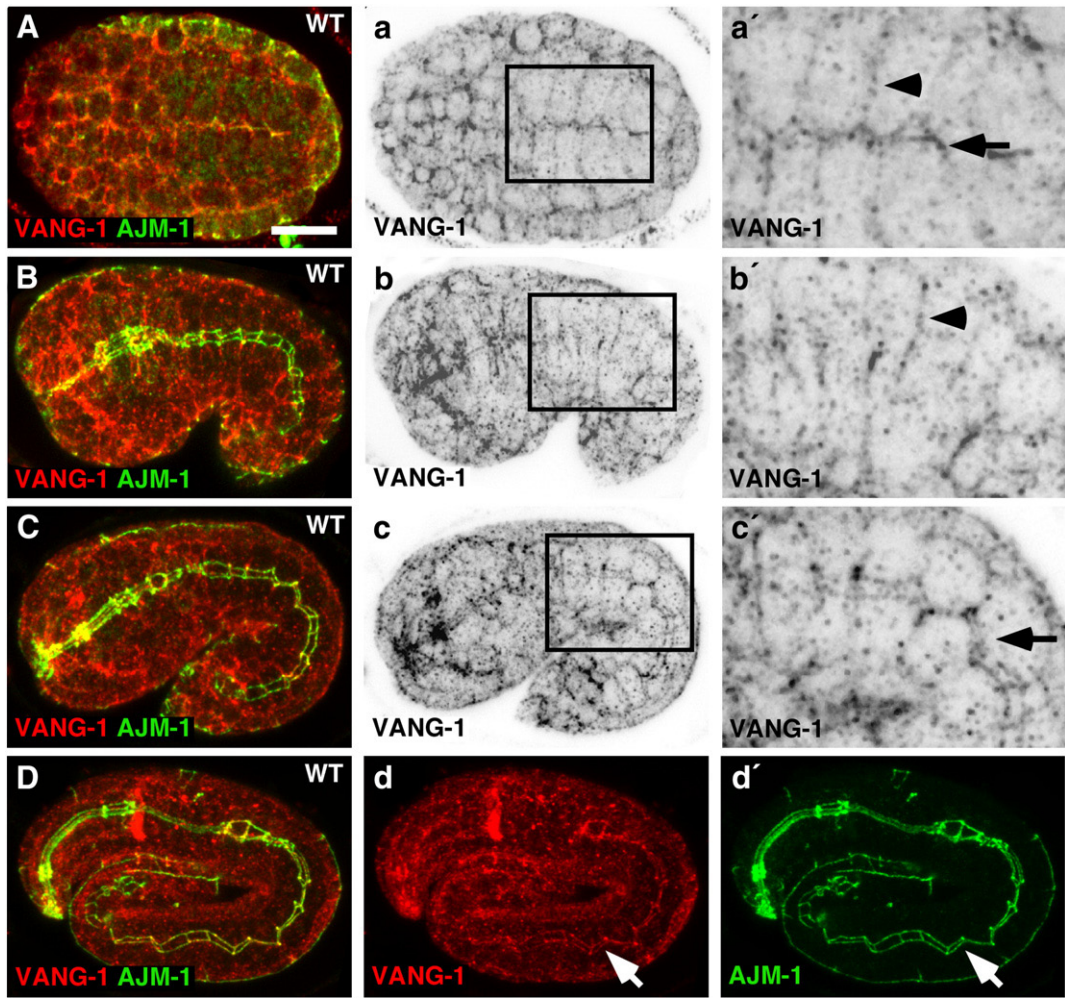


Fig. 3. VANG-1 displays a complex expression pattern during *Caenorhabditis elegans* embryogenesis. Double labeling of embryos with anti-VANG-1 (red) and mabMH27 (anti-AJM-1, green) antibodies. (A–D) Localization of VANG-1 during different phases of morphogenesis. (A–a′) At the end of the proliferation phase VANG-1 mostly localized at the lateral (arrowhead) and apical (arrow) membrane domains of intestinal cells (a′, arrowhead; $n = 20$). (B–b′) In early morphogenesis, VANG-1 was detectable at the lateral (arrow) but not apical membrane domain of the intestine ($n = 20$). (C–c′) In mid morphogenesis, VANG-1 appeared at the CeAJ (arrow), showing colocalization with the DAC ($n = 20$). (D–d′) In late morphogenesis, VANG-1 is still localized at the intestinal CeAJ (arrow; $n = 20$). Boxes (a–c) seen at higher magnification in (a′–c′), respectively. Orientation: anterior, left; dorsal, top. Scale bar: 10 μm .

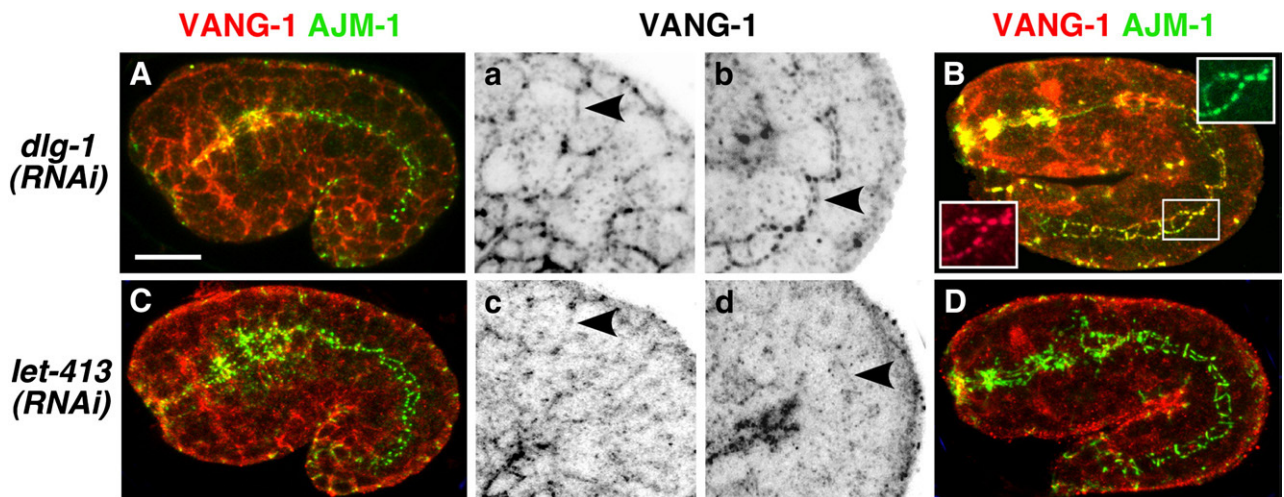


Fig. 4. The apical localization of VANG-1 in the intestine depends on DLG-1 and LET-413. Immunofluorescence of anti-VANG-1 antibodies (red) and mabMH27 (anti-AJM-1, green). (A, B) In *dlg-1(RNAi)* embryos, VANG-1 was detectable at the lateral membrane domain of intestinal cells (a, arrowhead) during early morphogenesis, while in mid morphogenesis clustering of VANG-1 and AJM-1 proteins became apparent at the CeAJ (b, arrowhead; see boxes for higher magnifications and note both proteins at the same apicolateral location). (C–D) In early morphogenesis, *let-413(RNAi)* embryos showed lateral distribution of VANG-1 (c, arrowhead). During mid morphogenesis, a faint staining of VANG-1 at the CeAJ became visible (d, arrowhead). (a–d) Higher magnification of intestinal cells, as seen in panels A–D. Orientation: anterior, left; dorsal, top. Scale bar: 10 μm .

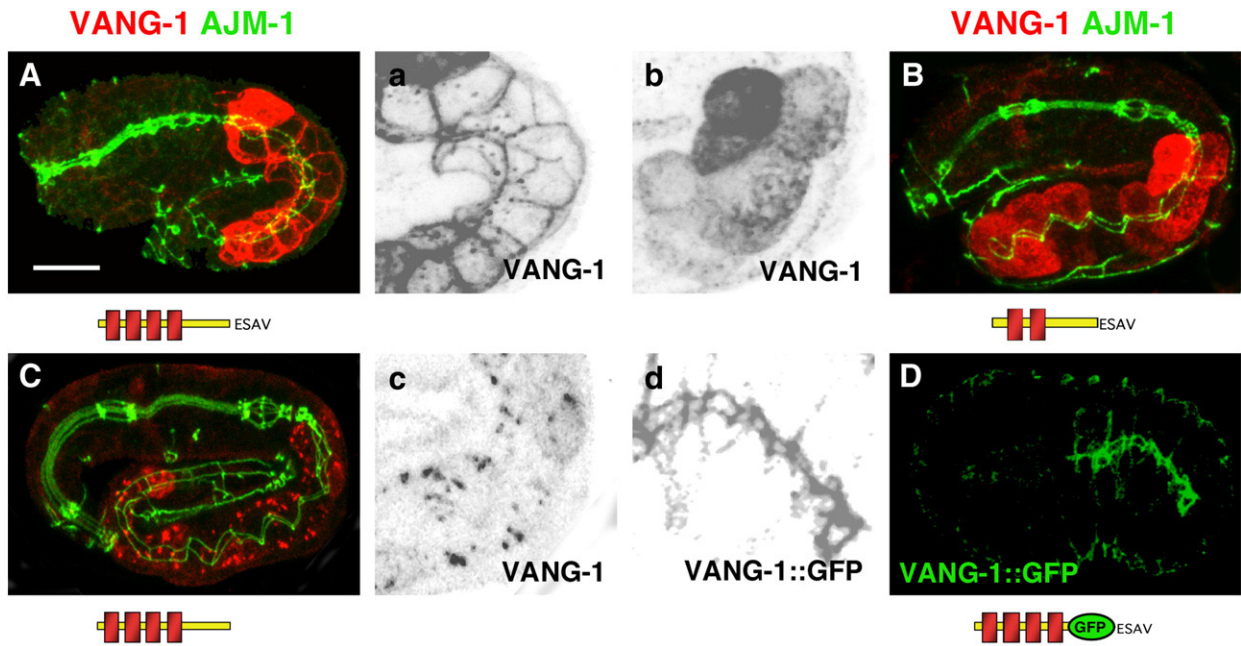


Fig. 5. Structure–function analysis of VANG-1. Immunofluorescence of VANG-1 (red), mabMH27 (anti-AJM-1, green) and the green fluorescent protein (GFP, d). VANG-1 constructs (see *Materials and methods* for details), used for intestine-specific overexpression under control of the *elt-2* promoter, are shown at the bottom of each picture (A–D, see Fig. 1 for color code). (A, a) Overexpression of full-length VANG-1 revealed cortical localization of the protein. (B, b) Overexpression of VANG-1, lacking the N terminus, revealed a diffuse cytoplasmic distribution. (C, c) Overexpression of VANG-1, missing the C-terminal PDZ domain binding motif (“–ESAV”, aa 529–533), displayed a granular staining in the cytoplasm, whereas no cortical VANG-1 staining was detectable. (D, d) The substitution of only the intracellular part of VANG-1 (aa 240–528) with GFP but leaving the “–ESAV” motif in its position led to premature redistribution of VANG-1 to the CeAJ (compare to Figs. 3c and C). Note, due to the bright fluorescence caused by overexpression of VANG-1, endogenous VANG-1 was not detectable in A–c. Orientation: anterior, left; dorsal, top. Scale bar: 10 μ m.

extends from the apical to the more lateral membrane domain, suggesting that the subcellular redistribution of Strabismus/Van Gogh/VANG-1 proteins during morphogenesis is conserved between species (Bellaiche et al., 2004).

Proper junctional localization of VANG-1 depends on DLG-1 and LET-413

Our interaction studies and immunofluorescence analysis (Figs. 2 and 3) both suggest that VANG-1 and DLG-1 functionally interact with each other. To test whether the junctional localization of VANG-1 really depends on DLG-1 function, we performed RNAi

against *dlg-1*. While in early morphogenesis of *dlg-1(RNAi)* embryos basolateral expression of VANG-1 is unaffected (Figs. 4A–a, arrowhead), in late morphogenesis anti-VANG-1 staining of the CeAJ no longer appears homogeneously around the apex of intestinal cells (Figs. 4B–b, arrowhead). Instead, a spotted VANG-1 expression pattern becomes apparent that is reminiscent to the distribution of AJM-1 in *dlg-1(RNAi)* embryos (Bossinger et al., 2001; Lockwood et al., 2008; McMahon et al., 2001; Segbert et al., 2004). Interestingly, most VANG-1 spots still contain AJM-1, suggesting similar behavior of both proteins after depletion of DLG-1 (see higher magnifications in Fig. 4B).

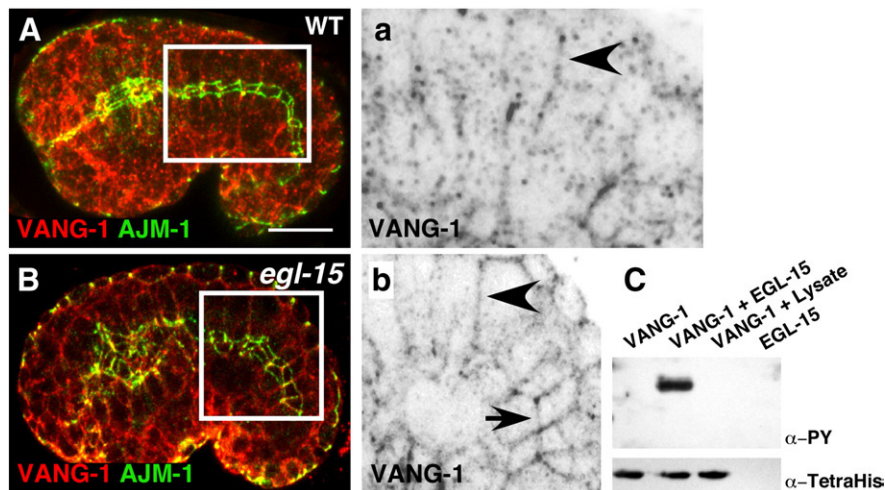


Fig. 6. The subcellular localization of VANG-1 depends on EGL-15. (A, B) Double stainings with anti-VANG-1 (red) and mabMH27 (anti-AJM-1, green) antibodies. (A) In mid morphogenesis of WT embryos VANG-1 was localized laterally but not apically in the intestinal cells (a, arrow). (B) In mid morphogenesis of *egl-15(n1456)* embryos, VANG-1 was distributed laterally (b, arrow) and apically (b, arrowhead) in intestinal cells. The organization of intestinal rings (see Fig. 7 for further details) was affected in comparison to WT. (C) The tyrosine kinase domain of EGL-15 was able to phosphorylate the VANG-1 C terminus *in vitro*. Bacterially expressed and purified His-tagged C terminus of VANG-1 was phosphorylated by *in vitro* translated EGL-15 kinase domain using reticulocyte lysate. Phosphorylation was detected with an anti-phosphotyrosine antibody. An anti-tetra His antibody was used in this assay to stain the input control of the VANG-1 C terminus. Orientation (A–b): anterior, left; dorsal, top. Scale bar: 10 μ m.

During epithelial development in *C. elegans*, correct localization of the DAC depends on basolaterally expressed LET-413 (Legouis et al., 2000; Legouis et al., 2003). Hence, we tested further genetic interactions and analyzed the distribution of VANG-1 after depletion of LET-413. In *let-413(RNAi)* embryos, the basolateral (“early”) anti-VANG-1 signal is still visible (Figs. 4C–c, arrowhead) but not the (“late”) junctional signal (Figs. 4D–d, arrowhead).

We conclude that DLG-1 and LET-413 are required for correct junctional localization of VANG-1. Genetic interactions of *let-413/Scrb1* and *vang-1/Vangl2* homologs in mammals have been reported (Moncouquiol et al., 2003). *Scrb1* displays four PDZ domains and a combination

of either two PDZ domains is sufficient to bind to the PDZ binding motif of Vangl2 (Kallay et al., 2006). In *C. elegans*, LET-413 only contains one PDZ domain and a direct association of LET-413 with the PDZ binding motif of VANG-1 has not been reported or predicted so far (Chen et al., 2008; Tonikian et al., 2008).

Recruitment of VANG-1 to the cell membrane requires its PDZ binding motif and depends on the FGF-like receptor tyrosine kinase EGL-15

The interaction of VANG-1 with DLG-1 occurs via its C-terminal PDZ binding motif (“–ESAV”, Fig. 1), but surprisingly depletion of

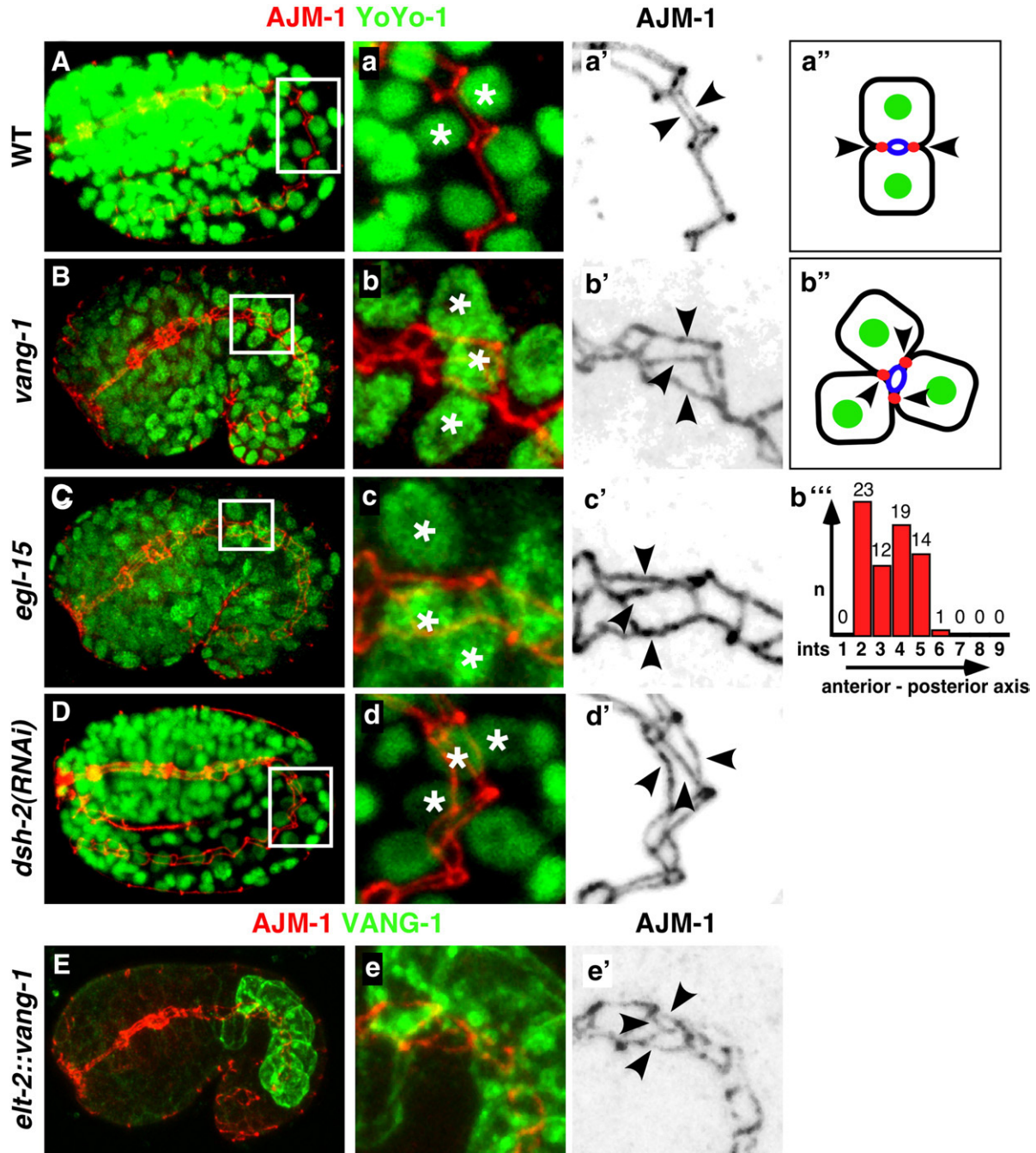


Fig. 7. Comparison of the CeAJ pattern during morphogenesis of *Caenorhabditis elegans* WT, *vang-1(tm1422)*, *egl-15(n1456)* and *dsh-2(RNAi)* embryo. Immunofluorescence of AJM-1 (red) and staining of DNA (YoYo-1, green) in *C. elegans* morphogenesis stages. (A) In WT embryos intestinal rings (“ints” II-IX; Leung et al., 1999) were formed by two epithelial cells (a, asterisk), which enclose a common lumen (a'', blue) and are connected by the apical junction (a', arrowheads; a'', red). (B) In *vang-1* embryos, “ints” were formed of three epithelial cells (b, asterisk; b'') connected by the CeAJ (b', arrowheads). In *vang-1* embryos ($n = 69$), defects in the formation of “ints” predominantly affected “ints” II–VI (b''). (C–E) Similar phenotypes were also observed in *egl-15* embryos (C, c), after depletion of DSH-2 (D, d) and after intestine-specific overexpression of *gfp::vang-1* C terminus (E–e'; see Materials and methods for details). Orientation: anterior, left; dorsal, top. Scale bar: 10 μ m.

DLG-1 by RNAi does not interfere with the basolateral or apical recruitment of VANG-1 to the cell membrane, as demonstrated by immunofluorescence analysis (see Figs. 4a and b). To test which role the PDZ binding motif plays for the correct localization and to identify other putative regulatory sequences, we performed a structure–function analysis of VANG-1 protein. Therefore, different *vang-1* constructs (Fig. 5) were cloned and overexpressed under the control of the intestine-specific *elt-2* promoter (Fukushige et al., 1998, 1999; Hawkins and McGhee, 1995).

Intestinal overexpression of full-length VANG-1 shows a clear signal at the plasma membrane (Figs. 5A–a). In contrast, overexpression of a construct missing the N terminus of VANG-1 (including a putative signal peptide and the first two transmembrane domains) reveals a diffuse cytoplasmic distribution in intestinal cells (Figs. 5B–b). After removing the C-terminal PDZ binding motif “–ESAV”, localization of VANG-1 at the cell membrane is completely abolished. Instead, VANG-1 becomes enriched in cytoplasmic granules (Figs. 5C–c) suggesting that the “–ESAV” motif is absolutely necessary for membrane localization and that other proteins beside DLG-1 and LET-413 are probably involved in the cortical recruitment of VANG-1.

To identify additional putative regulatory sequences of VANG-1, we replaced the intracellular domain with GFP and added the “–ESAV” motif to ensure proper localization at the plasma membrane

(Fig. 5D). While endogenous VANG-1 localizes basolaterally during early morphogenesis (see Fig. 3B) and becomes junctionally enriched later in development (see Fig. 3D), substitution of the intracellular part by GFP + “–ESAV” causes early junctional localization (Figs. 5d–D). Hence, we conclude that the intracellular domain of VANG-1 contains further control elements, that are required for proper time-dependent subcellular distribution.

To identify these control elements, we examined the intracellular domain of VANG-1 with regard to putative phosphorylation sites. By using the NetPhos 2.0 program (<http://www.cbs.dtu.dk/services/NetPhos/>) (Blom et al., 1999), three tyrosine residues (aa pos. 278, 313 and 414) were predicted to become phosphorylated (Fig. 1D). The latter phosphorylation site at the C terminus of VANG-1 shows a similar amino acid composition (RIGGY) to a known phosphorylation site (FIGQY) described in the *C. elegans* L1CAM homolog LAD-1 (Chen et al., 2001). Phosphorylation of LAD-1 requires the FGF-like receptor tyrosine kinase EGL-15 (Chen et al., 2001), which to our surprise had also been isolated in our Y2HA of DLG-1 (Fig. S1).

To test whether EGL-15 directly regulates VANG-1 by phosphorylation, we carried out an *in vitro* kinase assay and showed that the kinase domain of EGL-15 is able to phosphorylate the intracellular domain of VANG-1 (Fig. 6C). As previously reported, immunofluorescence did not detect endogenous EGL-15 in WT and *egl-15::gfp* expression in larval

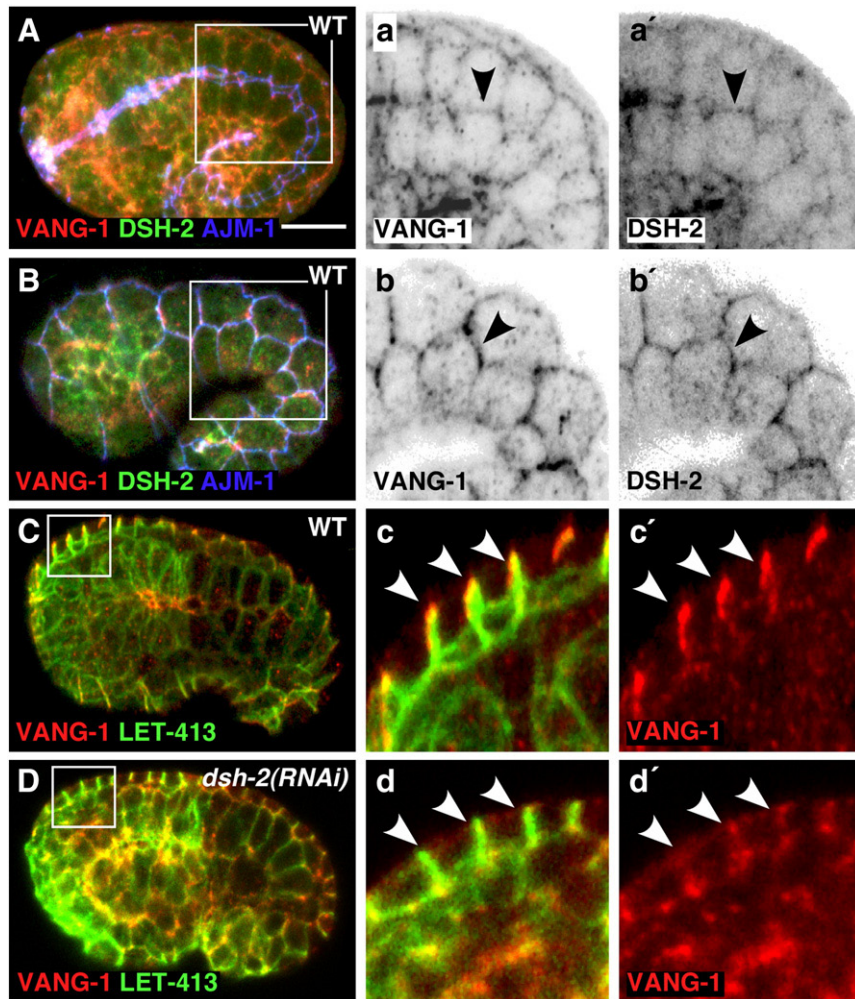


Fig. 8. The localization of VANG-1 depends on DSH-2. (A, B) Triple stainings with anti-VANG-1 (red), anti-DSH-2 (green) and mabMH27 (anti-AJM-1, blue). (C, D) Double stainings with anti-VANG-1 (red) and anti-GFP (green) in transgenic embryos expressing LET-413-GFP fusion protein. (A–b') Mid-morphogenesis stage showing intestinal (A–a') and hypodermal (B–b') distribution of VANG-1 (a, b arrowhead) and DSH-2 (a', b' arrowhead) at the cellular apex together with AJM-1. Note faint lateral stainings of VANG-1 and DSH-2 proteins (a, a'). (C) In the dorsal hypodermis, anterior cells showed an asymmetric distribution of VANG-1 at the posterior cortex (c, c', arrowheads). (D) The asymmetric distribution of VANG-1 in dorsal hypodermal cells disappeared after depletion of DSH-2 (d, d' arrowheads). Images in panels C and D were taken with single confocal scans. Orientation: anterior, left; dorsal, top. Scale bar: 10 μm.

stage animals was only described in the hypodermis (Bülow et al., 2004; Huang and Stern, 2004). To investigate whether the phosphorylation of VANG-1 by EGL-15 is a prerequisite for proper subcellular localization *in vivo*, we analyzed the distribution of VANG-1 in *egl-15* (*n1456*) embryos. During early morphogenesis of WT comma stage VANG-1 predominantly localizes at the basolateral membrane domain of intestinal cells (Figs. 6A–a). In contrast, in *egl-15*(*n1456*) embryos, basolaterally expressed VANG-1 became prematurely redistributed to the CeAJ (Figs. 6B–b).

Taken together, these results give further support for the idea that the C terminus of VANG-1 contains regulatory elements that seem to control the subcellular distribution of VANG-1 during morphogenesis of the *C. elegans* intestine.

vang-1 and *egl-15* affect morphogenesis of intestinal cells

To identify putative phenotypes in the intestine of *vang-1* (*tm1422*) and *egl-15*(*n1456*) embryos, we stained the DAC and DNA, using mab-MH27 against AJM-1 and the fluorescent dye YoYo-1, respectively (Fig. 7). In WT, the intestine is composed of nine rings of epithelial cells (called int I–IX), which surround the common lumen and are connected by the CeAJ (Bossinger et al., 2001, 2004; Hüskén et al., 2008; Leung et al., 1999; Sulston et al., 1983). While int I consists of four symmetrical cells, all other ints only contain two. The typical arrangement of intestinal cells is also illustrated by the “ladder-like” junctional pattern (see Figs. 7A–a”), which has been described previously (Bossinger et al., 2001; Leung et al., 1999; Podbilewicz and White, 1994). Careful examinations of *vang-1* (*tm1422*) and *egl-15*(*n1456*) embryos revealed intestines, where ints were made up of three epithelial cells instead of two (Figs. 7A–c’). A detailed analysis of *vang-1*(*tm1422*) embryos then uncovered the anterior part of the intestine (int II–VI) showing a high frequency of this phenotype (Fig. 7b’; *n* = 69/214). Interestingly, we noticed a similar phenotype after intestine-specific overexpression of full-length VANG-1 (Figs. 7E–e’). In *egl-15*(*n1456*) embryos, in which VANG-1 arrives prematurely at the CeAJ (see Figs. 6B–b), we observed a similar phenotype (Figs. 7C–c’; *n* = 34/133). In contrast, in WT, *dlg-1* and *let-413* RNAi embryos the defects in the formation of intestinal rings were not observed, as judged by immunofluorescence analysis (*n* > 50, each; see Figs. 4 and 7A). Thus, *vang-1* and *egl-15* mutant embryos display similar phenotypes in the *C. elegans* embryonic intestine. In addition, the subcellular localization of VANG-1 depends on EGL-15. Both observations indicate a crosstalk of VANG-1 and the FGF (EGL-15) signaling pathway in *C. elegans*. Recent findings in *Xenopus* also affiliate PCP and FGF signaling, suggesting a more general connection of both pathways in organogenesis (Lee et al., 2009; Shi et al., 2009).

The localization of VANG-1 depends upon DSH-2

During morphogenesis, VANG-1 shows a complex subcellular localization pattern in the embryonic intestine of *C. elegans* (see Fig. 3), which seems typical for PCP proteins in other systems (e.g. *Drosophila*) and is crucial for their functions (Axelrod and McNeill, 2002; Bastock et al., 2003; Strutt, 2001, 2008; Wu and Mlodzik, 2009).

Another key player in the PCP pathway is the PDZ domain containing protein Dishevelled (Wodarz and Nusse, 1998). In *Drosophila* and vertebrates, Dishevelled and Strabismus/Van Gogh phenotypes are similar (Doudney and Stanier, 2005). To test if Dishevelled is indeed required for intestinal morphogenesis, we analyzed the RNAi phenotypes of the known Dishevelled homologs, DSH-1, DSH-2 and MIG-5, which are involved in asymmetric cell divisions in *C. elegans* (Chang et al., 2005; Hawkins et al., 2005; Hingwing et al., 2009; King et al., 2009; Korswagen, 2002; Walston et al., 2006; Wu and Herman, 2007). While depletion of DSH-1 or MIG-5 does not affect morphogenesis of the intestine (not shown), *dsh-2*(RNAi) induced similar

phenotypes (Figs. 7D–d’) as observed in the intestines of *vang-1* (*tm1422*) and *egl-15*(*n1456*) embryos.

Because VANG-1 and DSH-2 show a clear colocalization in intestinal and hypodermal cells (Figs. 8A–b’) and the C terminus of VANG-1 interacts with the PDZ domain of DSH-2 in our Y2HA (Fig. S6), we analyzed the distribution of VANG-1 in *dsh-2*(RNAi) embryos. Using LET-413::CFP as a basolateral marker of epithelial cells in *C. elegans* (Legouis et al., 2000), we noticed an asymmetric distribution of VANG-1 to the posterior membrane of some epithelial cells in WT (Figs. 8C–c’) that either completely disappeared or became diminished after *dsh-2* RNAi (Figs. 8D–d’). Taken together, the subcellular distribution of VANG-1 in the *C. elegans* embryonic intestine is directly modulated by LET-413, DLG-1 and DSH-2 and depends on FGF-like receptor tyrosine kinase EGL-15 (Fig. 9).

The asymmetric distribution of a large protein scaffold along the plane of the epithelial cell layer (perpendicular to the apical-basal axis) is the hallmark of the PCP in other systems (Tree et al., 2002) and seems to be conserved in *C. elegans*. The oriented cell division and allocation of the divided cells along the cell division axis contribute to organ lengthening in the *C. elegans* intestine (Leung et al., 1999). Basically the E-blastomere, the founder cell of the *C. elegans* intestine, divides along the anterior–posterior axis. At the E¹⁶ stage, a set of four intestinal cells intercalate along the dorso-ventral axis at distinct entry sites, thus finishing the assembly of the epithelial monolayer, which later form an epithelial tube.

Defects in cell intercalation or polarized cell division have not been described in the *C. elegans* intestine, so far. In *vang-1* embryos, intestinal patterning is impaired within a distinct domain along the anterior–posterior axis. In line with our observation, the participation of *vang-1* homologs in cell intercalation processes during organ formation is well established (Axelrod and McNeill, 2002; Darken et al., 2002). Additionally, roles for PCP signaling concerning the polarization of cells along the anterior–posterior axis have been described (Ciruna et al., 2006). Recent findings demonstrate that oriented or asymmetric cell divisions in the developing gut epithelium of the zebrafish in the mouse brain and in *Drosophila*

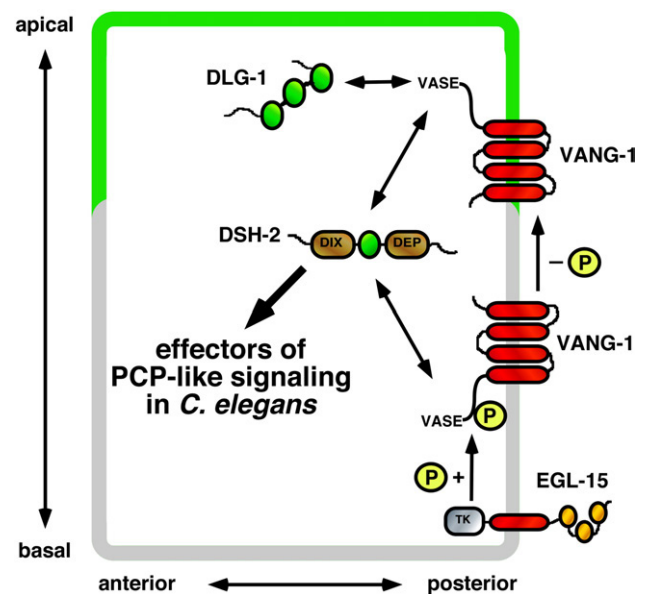


Fig. 9. Working model of *vang-1* function in the *Caenorhabditis elegans* embryo. Phosphorylation of asymmetric distributed planar cell polarity protein VANG-1 (transmembrane domains in red) by FGF-like receptor tyrosine kinase orthologue EGL-15 ensures basolateral position in epithelial cells. Dephosphorylation of VANG-1 by a so far unknown phosphatase leads to an apical shift in position where the protein interacts with DLG-1 (PDZ domains in green), a structural component of the CeAJ. Interaction of VANG-1 with Dishevelled related protein DSH-2, an effector of PCP-like signaling, can either occur at the basolateral membrane domain or at the CeAJ.

sensory organ precursor cells is regulated by PCP signaling (Gomes et al., 2009; Lake and Sokol, 2009; Matsuyama et al., 2009). Hence, in the *C. elegans* intestine defects in oriented cell division or cell intercalation might contribute to the *vang-1* phenotype. Because of the spatial restriction to the anterior part, a defect in cell intercalation the most likely explanation is.

A PCP-like pathway has been postulated in *C. elegans*, in which LIN-17/Frizzled and MIG-5/Dishevelled are asymmetrically localized during the regulation of B cell polarity (Wu and Herman, 2006, 2007). This study introduces VANG-1 as another key player (Fig. 9) and hence provides further evidence concerning the existence of PCP-like signaling in *C. elegans*.

Acknowledgments

The authors would like to thank Z. Zhou (Horvitz lab) for providing embryonic cDNA library, J. McGhee for providing *elt-2* promoter construct, the Mitani lab for providing *tm1422*, N. Hawkins for providing antibodies, Y. Kohara, M. Labouesse and A. Wodarz for providing cDNA clones and R. Windoffer for critical comments on the manuscript. Some nematode strains used in this work were provided by the *Caenorhabditis* Genetics Center, which is funded by the NIH National Center for Research Resources (NCR). C.S. was funded by a fellowship from the Boehringer Ingelheim Fonds. This work was supported of a grant of the DFG to O.B.

Appendix A. Supplementary data

Supplementary data associated with this article can be found, in the online version, at doi:10.1016/j.ydbio.2009.12.002.

References

- Axelrod, J., McNeill, H., 2002. Coupling planar cell polarity signaling to morphogenesis. *ScientificWorldJournal* 2, 434–454.
- Bastock, R., Strutt, H., Strutt, D., 2003. Strabismus is asymmetrically localised and binds to Prickle and Dishevelled during *Drosophila* planar polarity patterning. *Development* 130, 3007–3014.
- Bellaïche, Y., Beaudoin-Massiani, O., Stuttem, I., Schweisguth, F., 2004. The planar cell polarity protein Strabismus promotes Pins anterior localization during asymmetric division of sensory organ precursor cells in *Drosophila*. *Development* 131, 469–478.
- Bertet, C., Sulak, L., Lecuit, T., 2004. Myosin-dependent junction remodelling controls planar cell intercalation and axis elongation. *Nature* 429, 667–671.
- Blom, N., Gammeltoft, S., Brunak, S., 1999. Sequence and structure-based prediction of eukaryotic protein phosphorylation sites. *J. Mol. Biol.* 294, 1351–1362.
- Bossinger, O., Klebes, A., Segbert, C., Theres, C., Knust, E., 2001. Zonula adherens formation in *Caenorhabditis elegans* requires *dlg-1*, the homologue of the *Drosophila* gene discs large. *Dev. Biol.* 230, 29–42.
- Bossinger, O., Fukushige, T., Claeys, M., Borgonie, G., McGhee, J.D., 2004. The apical disposition of the *Caenorhabditis elegans* intestinal terminal web is maintained by LET-413. *Dev. Biol.* 268, 448–456.
- Brenner, S., 1974. The genetics of *Caenorhabditis elegans*. *Genetics* 77, 71–94.
- Bülow, H.E., Boulin, T., Hobert, O., 2004. Differential functions of the *C. elegans* FGF receptor in axon outgrowth and maintenance of axon position. *Neuron* 42, 367–374.
- Carberry, K., Wiesenfahrt, T., Windoffer, R., Bossinger, O., Leube, R.E., 2009. Intermediate filaments in *Caenorhabditis elegans*. *Cell Motil. Cytoskeleton* 66, 852–864.
- Chang, W., Lloyd, C.E., Zarkower, D., 2005. DSH-2 regulates asymmetric cell division in the early *C. elegans* somatic gonad. *Mech. Dev.* 122, 781–789.
- Chen, L., Ong, B., Bennett, V., 2001. LAD-1, the *Caenorhabditis elegans* L1CAM homologue, participates in embryonic and gonadal morphogenesis and is a substrate for fibroblast growth factor receptor pathway-dependent phosphotyrosine-based signaling. *J. Cell. Biol.* 154, 841–855.
- Chen, J.R., Chang, B.H., Allen, J.E., Stiffler, M.A., Macbeath, G., 2008. Predicting PDZ domain-peptide interactions from primary sequences. *Nat. Biotechnol.* 26, 1041–1045.
- Ciruna, B., Jenny, A., Lee, D., Mlodzik, M., Schier, A.F., 2006. Planar cell polarity signalling couples cell division and morphogenesis during neurulation. *Nature* 439, 220–224.
- Darken, R.S., Scola, A.M., Rakeman, A.S., Das, G., Mlodzik, M., Wilson, P.A., 2002. The planar polarity gene strabismus regulates convergent extension movements in *Xenopus*. *EMBO J.* 21, 976–985.
- Doudney, K., Stanier, P., 2005. Epithelial cell polarity genes are required for neural tube closure. *Am. J. Med. Genet. C Semin. Med. Genet.* 135, 42–47.
- Fukushige, T., Hawkins, M.G., McGhee, J.D., 1998. The GATA-factor *elt-2* is essential for formation of the *Caenorhabditis elegans* intestine. *Dev. Biol.* 198, 286–302.
- Fukushige, T., Hendzel, M.J., Bazett-Jones, D.P., McGhee, J.D., 1999. Direct visualization of the *elt-2* gut-specific GATA factor binding to a target promoter inside the living *Caenorhabditis elegans* embryo. *Proc. Natl. Acad. Sci. U. S. A.* 96, 11883–11888.
- Gomes, J.E., Corado, M., Schweisguth, F., 2009. Van Gogh and Frizzled act redundantly in the *Drosophila* sensory organ precursor cell to orient its asymmetric division. *PLoS ONE* 4, e4485.
- Goto, T., Keller, R., 2002. The planar cell polarity gene strabismus regulates convergence and extension and neural fold closure in *Xenopus*. *Dev. Biol.* 247, 165–181.
- Green, J., Inoue, T., Sternberg, P., 2008. Opposing Wnt pathways orient cell polarity during organogenesis. *Cell* 134, 646–656.
- Hawkins, M., McGhee, J., 1995. *elt-2*, a second GATA factor from the nematode *Caenorhabditis elegans*. *J. Biol. Chem.* 270, 14666–14671.
- Hawkins, N.C., Ellis, G.C., Bowerman, B., Garriga, G., 2005. MOM-5 frizzled regulates the distribution of DSH-2 to control *C. elegans* asymmetric neuroblast divisions. *Dev. Biol.* 284, 246–259.
- Hermann, G.J., Leung, B., Priess, J.R., 2000. Left-right asymmetry in *C. elegans* intestine organogenesis involves a LIN-12/Notch signaling pathway. *Development* 127, 3429–3440.
- Hingwing, K., Lee, S., Nykilchuk, L., Walston, T., Hardin, J., Hawkins, N., 2009. CWN-1 functions with DSH-2 to regulate *C. elegans* asymmetric neuroblast division in a beta-catenin independent Wnt pathway. *Dev. Biol.* 328, 245–256.
- Huang, P., Stern, M.J., 2004. FGF signaling functions in the hypodermis to regulate fluid balance in *C. elegans*. *Development* 131, 2595–2604.
- Hüsken, K., Wiesenfahrt, T., Abraham, C., Windoffer, R., Bossinger, O., Leube, R., 2008. Maintenance of the intestinal tube in *Caenorhabditis elegans*: the role of the intermediate filament protein IFC-2. *Differentiation* 76, 881–896.
- Kallay, L.M., McNickle, A., Brennwald, P.J., Hubbard, A.L., Braiterman, L.T., 2006. Scribble associates with two polarity proteins, Lgl2 and Vangl2, via distinct molecular domains. *J. Cell. Biochem.* 99, 647–664.
- Keller, R., 2002. Shaping the vertebrate body plan by polarized embryonic cell movements. *Science* 298, 1950–1954.
- Keller, R., Shook, D., Skoglund, P., 2008. The forces that shape embryos: physical aspects of convergent extension by cell intercalation. *Phys. Biol.* 5, 15007.
- Kibar, Z., Vogan, K.J., Groulx, N., Justice, M.J., Underhill, D.A., Gros, P., 2001. *Itap*, a mammalian homolog of *Drosophila* Strabismus/Van Gogh, is altered in the mouse neural tube mutant Loop-tail. *Nat. Genet.* 28, 251–255.
- King, R.S., Maiden, S.L., Hawkins, N.C., Kidd 3rd, A.R., Kimble, J., Hardin, J., Walston, T.D., 2009. The N- or C-terminal domains of DSH-2 can activate the *C. elegans* Wnt/beta-catenin asymmetry pathway. *Dev. Biol.* 328, 234–244.
- Korswagen, H., 2002. Canonical and non-canonical Wnt signaling pathways in *Caenorhabditis elegans*: variations on a common signaling theme. *Bioessays* 24, 801–810.
- Krogh, A., Larsson, B., von Heijne, G., Sonnhammer, E.L., 2001. Predicting transmembrane protein topology with a hidden Markov model: application to complete genomes. *J. Mol. Biol.* 305, 567–580.
- Kuchinke, U., Grawe, F., Knust, E., 1998. Control of spindle orientation in *Drosophila* by the Par-3-related PDZ-domain protein Bazooka. *Curr. Biol.* 8, 1357–1365.
- Labouesse, M., 2006. Epithelial junctions and attachments. *WormBook*.
- Lake, B.B., Sokol, S.Y., 2009. Strabismus regulates asymmetric cell divisions and cell fate determination in the mouse brain. *J. Cell. Biol.* 185, 59–66.
- Lee, O.K., Frese, K.K., James, J.S., Chadda, D., Chen, Z.H., Javier, R.T., Cho, K.O., 2003. Discs-large and strabismus are functionally linked to plasma membrane formation. *Nat. Cell. Biol.* 5, 987–993.
- Lee, H.S., Mood, K., Battu, G., Ji, Y.J., Singh, A., Daar, I.O., 2009. Fibroblast growth factor receptor-induced phosphorylation of ephrinB1 modulates its interaction with Dishevelled. *Mol. Biol. Cell.* 20, 124–133.
- Legouis, R., Gansmuller, A., Sookharea, S., Boshier, J.M., Baillie, D.L., Labouesse, M., 2000. LET-413 is a basolateral protein required for the assembly of adherens junctions in *Caenorhabditis elegans*. *Nat. Cell. Biol.* 2, 415–422.
- Legouis, R., Jaulin-Bastard, F., Schott, S., Navarro, C., Borg, J.P., Labouesse, M., 2003. Basolateral targeting by leucine-rich repeat domains in epithelial cells. *EMBO Rep.* 4, 1096–1100.
- Leung, B., Hermann, G.J., Priess, J.R., 1999. Organogenesis of the *Caenorhabditis elegans* intestine. *Dev. Biol.* 216, 114–134.
- Lockwood, C.A., Lynch, A.M., Hardin, J., 2008. Dynamic analysis identifies novel roles for DLG-1 subdomains in AJM-1 recruitment and LET-413-dependent apical focusing. *J. Cell. Sci.* 121, 1477–1487.
- Lynch, A.M., Hardin, J., 2009. The assembly and maintenance of epithelial junctions in *C. elegans*. *Front. Biosci.* 14, 1414–1432.
- Matsuyama, M., Aizawa, S., Shimono, A., 2009. Sfrp controls apicobasal polarity and oriented cell division in developing gut epithelium. *PLoS Genet.* 5, e1000427.
- McGhee, J.D., 2007. The *C. elegans* intestine. *WormBook*.
- McMahon, L., Legouis, R., Vonesch, J.L., Labouesse, M., 2001. Assembly of *C. elegans* apical junctions involves positioning and compaction by LET-413 and protein aggregation by the MAGUK protein DLG-1. *J. Cell. Sci.* 114, 2265–2277.
- Montcouquiol, M., Rachel, R., Lanford, P., Copeland, N., Jenkins, N., Kelley, M., 2003. Identification of Vangl2 and Scrib1 as planar polarity genes in mammals. *Nature* 423, 173–177.
- Park, F.D., Tenlen, J.R., Priess, J.R., 2004. *C. elegans* MOM-5/frizzled functions in MOM-2/Wnt-independent cell polarity and is localized asymmetrically prior to cell division. *Curr. Biol.* 14, 2252–2258.
- Podbilewicz, B., White, J., 1994. Cell fusions in the developing epithelia of *C. elegans*. *Dev. Biol.* 161, 408–424.
- Segbert, C., Johnson, K., Theres, C., van Firden, D., Bossinger, O., 2004. Molecular and functional analysis of apical junction formation in the gut epithelium of *Caenorhabditis elegans*. *Dev. Biol.* 266, 17–26.

- Shi, W., Peyrot, S.M., Munro, E., Levine, M., 2009. FGF3 in the floor plate directs notochord convergent extension in the *Ciona* tadpole. *Development* 136, 23–28.
- Songyang, Z., Fanning, A., Fu, C., Xu, J., Marfatia, S., Chishti, A., Crompton, A., Chan, A., Anderson, J., Cantley, L., 1997. Recognition of unique carboxyl-terminal motifs by distinct PDZ domains. *Science* 275, 73–77.
- Sonnhammer, E., Eddy, S., Birney, E., Bateman, A., Durbin, R., 1998. Pfam: multiple sequence alignments and HMM-profiles of protein domains. *Nucleic Acids Res.* 26, 320–322.
- Strome, S., Wood, W.B., 1983. Generation of asymmetry and segregation of germ-line granules in early *C. elegans* embryos. *Cell* 35, 15–25.
- Strutt, D., 2001. Asymmetric localization of frizzled and the establishment of cell polarity in the *Drosophila* wing. *Mol. Cell* 7, 367–375.
- Strutt, D., 2008. The planar polarity pathway. *Curr. Biol.* 18, R898–R902.
- Sulston, J., Schierenberg, E., White, J., Thomson, J., 1983. The embryonic cell lineage of the nematode *Caenorhabditis elegans*. *Dev. Biol.* 100, 64–119.
- Taylor, J., Abramova, N., Charlton, J., Adler, P.N., 1998. Van Gogh: a new *Drosophila* tissue polarity gene. *Genetics* 150, 199–210.
- Tonikian, R., Zhang, Y., Sazinsky, S.L., Currell, B., Yeh, J.H., Reva, B., Held, H.A., Appleton, B.A., Evangelista, M., Wu, Y., Xin, X., Chan, A.C., Seshagiri, S., Lasky, L.A., Sander, C., Boone, C., Bader, G.D., Sidhu, S.S., 2008. A specificity map for the PDZ domain family. *PLoS Biol.* e239, 6.
- Tree, D., Ma, D., Axelrod, J., 2002. A three-tiered mechanism for regulation of planar cell polarity. *Semin. Cell Dev. Biol.* 13, 217–224.
- Wallingford, J.B., Fraser, S.E., Harland, R.M., 2002. Convergent extension: the molecular control of polarized cell movement during embryonic development. *Dev. Cell* 2, 695–706.
- Walston, T., Guo, C., Proenca, R., Wu, M., Herman, M.A., Hardin, J., Hedgecock, E.M., 2006. mig-5/Dsh controls cell fate determination and cell migration in *C. elegans*. *Dev. Biol.* 298, 485–497.
- Wang, Y., Nathans, J., 2007. Tissue/planar cell polarity in vertebrates: new insights and new questions. *Development* 134, 647–658.
- Wodarz, A., Nusse, R., 1998. Mechanisms of Wnt signaling in development. *Annu. Rev. Cell. Dev. Biol.* 14, 59–88.
- Wodarz, A., Ramrath, A., Kuchinke, U., Knust, E., 1999. Bazooka provides an apical cue for Inscuteable localization in *Drosophila* neuroblasts. *Nature* 402, 544–547.
- Wolff, T., Rubin, G., 1998. Strabismus, a novel gene that regulates tissue polarity and cell fate decisions in *Drosophila*. *Development* 125, 1149–1159.
- Wu, M., Herman, M.A., 2006. A novel noncanonical Wnt pathway is involved in the regulation of the asymmetric B cell division in *C. elegans*. *Dev. Biol.* 293, 316–329.
- Wu, M., Herman, M.A., 2007. Asymmetric localizations of LIN-17/Fz and MIG-5/Dsh are involved in the asymmetric B cell division in *C. elegans*. *Dev. Biol.* 303, 650–662.
- Wu, J., Mlodzik, M., 2009. A quest for the mechanism regulating global planar cell polarity of tissues. *Trends Cell. Biol.* 19, 295–305.